Pain persists in mice lacking both Substance P and CGRPα signaling

Donald Iain MacDonald[1], Monessha Jayabalan[1], Jonathan Seaman[1], Alec Nickolls[1] and Alexander Chesler[1,2*]

[1]*National Center for Complementary and Integrative Health, National Institutes of Health, Bethesda, United States*

[2]*National Institute of Neurological Disorders and Stroke, National Institutes of Health, Bethesda, United States*

*Correspondence: alexander.chesler@nih.gov

Keywords: neuropeptides, Substance P, CGRP, nociception, chronic pain, neuropathic pain, inflammatory pain

Summary

The neuropeptides Substance P and CGRPα have long been thought important for pain sensation. Both peptides and their receptors are expressed at high levels in pain-responsive neurons from the periphery to the brain making them attractive therapeutic targets. However, drugs targeting these pathways individually did not relieve pain in clinical trials. Since Substance P and CGRPα are extensively co-expressed we hypothesized that their simultaneous inhibition would be required for effective analgesia. We therefore generated *Tac1* and *Calca* double knockout (DKO) mice and assessed their behavior using a wide range of pain-relevant assays. As expected, Substance P and CGRPα peptides were undetectable throughout the nervous system of DKO mice. To our surprise, these animals displayed largely intact responses to mechanical, thermal, chemical, and visceral pain stimuli, as well as itch. Moreover, chronic inflammatory pain and neurogenic inflammation were unaffected by loss of the two peptides. Finally, neuropathic pain evoked by nerve injury or chemotherapy treatment was also preserved in peptide-deficient mice. Thus, our results demonstrate that even in combination, Substance P and CGRPα are not required for the transmission of acute and chronic pain.

1. Introduction

Over a hundred neuropeptides are expressed by mammalian neurons (Russo, 2017). Neuropeptides are released through the secretory pathway and activate G-protein coupled receptors to control neuronal excitability and synaptic strength (Pagani et al., 2019). They can also influence the function of immune cells in peripheral tissues (Chiu et al., 2012). Drugs acting on neuropeptides or their receptors are now widely used in the clinic, including therapeutics for obesity and migraine (Drucker, 2022; Ogunlaja and Goadsby, 2022). Which peptides can be targeted successfully and for what indications thus remain key questions for neuroscience and drug development.

Among the most challenging diseases to treat is chronic pain. With over 20% of the population suffering from chronic pain, we urgently need to find new analgesic targets (Nahin et al., 2023). The two neuropeptides most strongly implicated in chronic pain are Substance P and CGRPα (De Matteis et al., 2020; Paige et al., 2022; Yaksh et al., 1980; Zieglgänsberger, 2019). Substance P is an 11-amino acid peptide first discovered as a tissue extract with contractile activity (von Euler and Gaddum, 1931). CGRPα is a 37-amino acid peptide and potent vasodilator identified as the alternatively spliced product of the calcitonin gene (Amara et al., 1982). Both Substance P and CGRPα are highly expressed in pain-responsive neurons throughout the nervous system. In the periphery, strong activation of nociceptor sensory neurons is reported to cause peptide secretion and neurogenic inflammation (Chiu et al., 2012). Similarly, release of Substance P and CGRPα in the spinal cord and brainstem may alter pain transmission in ascending pain pathways (Huang et al., 2019; Latremoliere and Woolf, 2009; Löken et al., 2021). In the brain, these molecules are prominently enriched in areas known to be involved in pain, including the periaqueductal grey, parabrachial nucleus and amygdala (Barik et al., 2018; Lein et al., 2007; Palmiter, 2018). Thus, decades of research implicate Substance P and CGRPα as critical drivers of pain, including modulating tissue inflammation, sensory hypersensitivity, pain chronification and unpleasantness (Chiu et al., 2012; De Matteis et al., 2020; Zieglgänsberger, 2019).

However, selective antagonists of the Substance P receptor NKR1 failed to relieve chronic pain in human clinical trials (Hill, 2000). Although CGRP monoclonal antibodies and receptor blockers have proven effective for subsets of migraine patients, their usefulness for other types of pain in humans is unclear (De Matteis et al., 2020; Jin et al., 2018). In line with this, knockout mice deficient in Substance P, CGRPα or their receptors have been reported to display some pain deficits,

68 but the analgesic effects are neither large nor consistent between studies (Cao et al., 1998; De Felipe
69 et al., 1998; Guo et al., 2012; Salmon et al., 2001, 1999; Zimmer et al., 1998).

70 By contrast, ablating or inhibiting peptidergic nociceptors causes profound decreases in heat
71 sensitivity, inflammatory heat hyperalgesia, and some forms of mechanical allodynia (Cowie et al.,
72 2018; McCoy et al., 2013). Mice with silenced Substance P or CGRPα-expressing neurons in brain
73 areas such as the parabrachial nucleus also show impaired pain behavior (Barik et al., 2018; Han et
74 al., 2015; Kang et al., 2022; Sun et al., 2020). In the periphery, Substance P and CGRPα are
75 expressed by largely the same nociceptors, in mice and in humans (Nguyen et al., 2021; Sharma et
76 al., 2020). The two peptides are also co-expressed in the brain (Pauli et al., 2022; Zeisel et al., 2018).
77 Redundancy is built into pain pathways because of their importance for survival and may explain
78 why attenuating the signaling of a single peptide does not recapitulate the analgesic effect of
79 silencing the cell secreting it (Vandewauw et al., 2018).

80 Given the well-described roles for peptidergic neurons in pain and the widespread co-
81 expression of Substance P and CGRPα, we reasoned that removal of both peptides should reveal
82 roles for peptidergic signaling that might be masked by redundancy. We therefore generated and
83 characterized *Tac1::Calca* double knockout (DKO) mice lacking both Substance P and CGRPα
84 peptides. We predicted these DKO animals might recapitulate the striking absence of inflammatory
85 pain observed in naked mole rats that release glutamate but not Substance P or CGRPα from
86 nociceptors (Park et al., 2008, 2003). Here we present a thorough evaluation of the impact of dual
87 peptide deletion on acute and chronic pain behavior in laboratory mice.

88

89

90 # 2. Results

91 ## 2.1. Double knockout mice completely lack Substance P and CGRPα signaling

92 To investigate the roles of Substance P and CGRPα in pain processing, we generated Tac1::Calca
93 Double Knockout (DKO) mice with constitutive deletion of the two peptide precursor genes. A
94 homozygous Tac1-RFP knockin-knockout line was used to remove the *Tac1* gene encoding
95 preprotachykinin, the precursor for Substance P and Neurokinin A (Wu et al., 2018). As expected,
96 no detectable Substance P immunostaining was observed in pain-relevant areas including the dorsal
97 root ganglion, dorsal horn of the spinal cord, parabrachial nucleus and periaqueductal gray (Figure
98 1A). To eliminate CGRPα signaling, we used a Calca-Cre mouse, which at homozygosity is a
99 knockout for the *Calca* gene encoding the Calcitonin and CGRPα peptides (Carter et al., 2013; Chen
100 et al., 2018). We were unable to detect CGRP immunoreactivity in DRG, spinal cord and the
101 amygdala (Figure 1B) validating the DKO approach.

102 A clear prediction from the loss of immunostaining is that sensory neuron activity should no
103 longer activate the Substance P receptor NKR1. We developed a cell-based assay to monitor NKR1
104 signaling by generating HEK293 cells stably expressing NKR1, GCaMP6s and Gα15 (so-called
105 'Substance P-sniffer' cells) (Figure 1C). These cells responded to low nanomolar concentrations of
106 Substance P (EC_{50}=11.8 nM, Figure 1 – figure supplement 1A). We reasoned that in co-cultures
107 with DRG neurons, application of the potent TRPV1 agonist capsaicin (10 μM) would stimulate
108 nociceptors to release Substance P and thereby activate neighboring Substance P-sniffer cells.
109 Control DRGs treated with capsaicin evoked robust GCaMP responses in surrounding Substance P-
110 sniffer cells (Figure 1D-E). In contrast, capsaicin stimulated DKO-DRG neurons induced no
111 Substance P-sniffer cell responses (Figure 1D-E). In combination, these experiments demonstrate
112 that deletion of *Tac1* completely blocks the endogenous activation of NKR1 receptors by nociceptor
113 neurons.

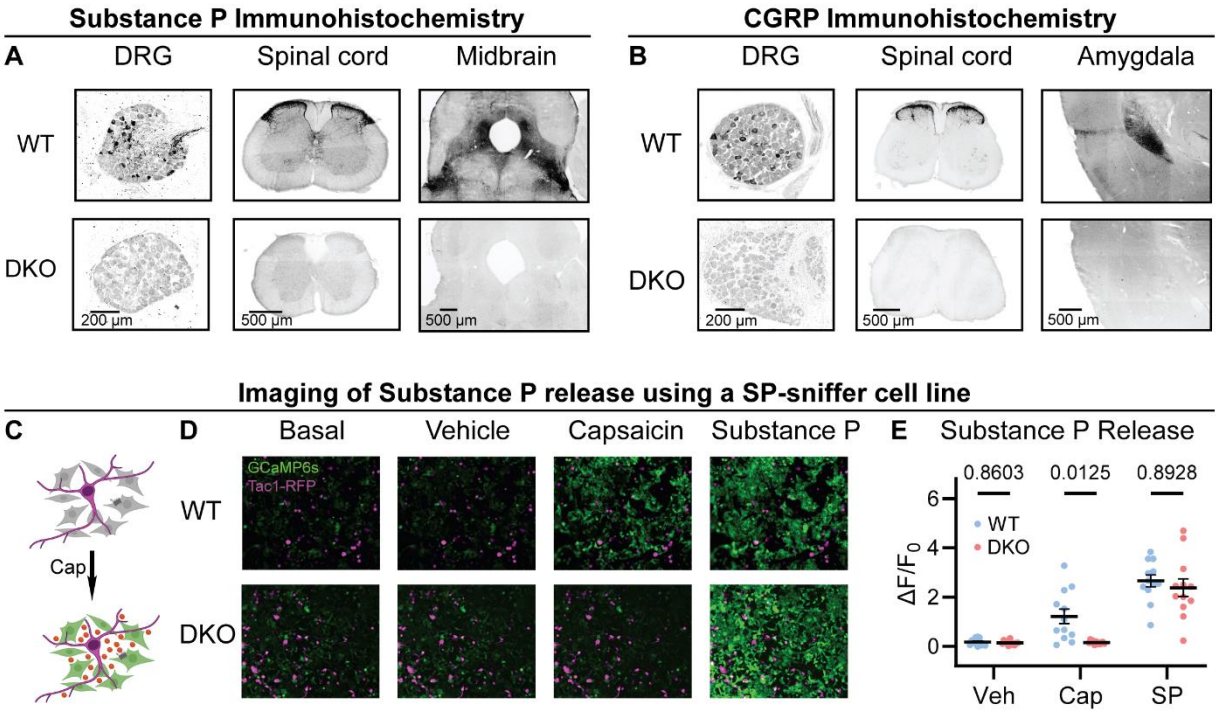

Figure 1. Tac1::Calca DKO mice lack Substance P and CGRPα peptides throughout the nervous system. (A) Confocal images showing Substance P immunostaining in the dorsal root ganglion (DRG), spinal cord dorsal horn and midbrain of a WT mouse (*top*). No staining is detectable in the DKO (*bottom*). **(B)** Confocal images showing CGRP immunostaining in the DRG, spinal cord dorsal horn, and amygdala of a WT mouse (*top*). The DKO mice show no obvious staining (*bottom*). Images in both (A) and (B) are representative of staining performed on tissue from 1M and 1F animal per genotype. **(C)** Schematic showing co-culture of Tac1-RFP-labelled DRG neurons and Substance P-sniffer HEK293 cells expressing NKR1, GCaMP6s and Gα15. Capsaicin-evoked secretion of Substance P from DRG activates the NKR1 receptor in neighboring HEK leading to calcium release from stores and GCaMP6s-mediated fluorescence increase. **(D)** Fluorescence images showing Tac1-RFP-labelled DRG neurons (*magenta*) and Substance P-sniffer cells. Capsaicin causes an increase in Substance P-sniffer GCaMP6s fluorescence (*green*) when cultured with DRGs from WT, but not DKO, mice. Application of exogenous Substance P (10 nM) activates Substance P-sniffers in both conditions. **(E)** Quantification of fluorescence change in Substance P-sniffer cells in response to vehicle, capsaicin and Substance P stimulation in WT and DKO mice. n=12 chambers from 2 mice (1M, 1F) for WT, and n=12 chambers from 2 mice (1M, 1F) for DKO. For (E), means were compared using repeated measures 2-way ANOVA, followed by post-hoc Sidak's test. Error bars denote standard error of the mean.

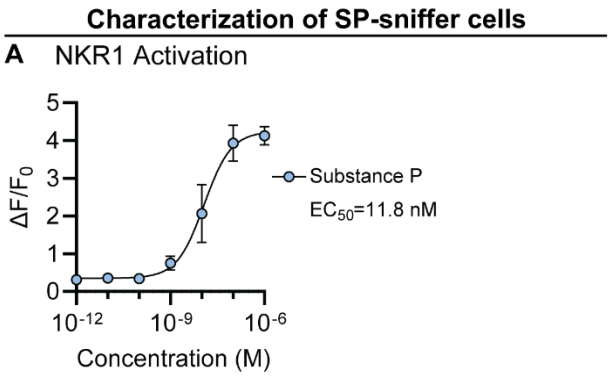

Figure 1 – figure supplement 1. Substance P-sniffer cells selectively respond to Substance P in an NKR1-dependent manner. (A) Dose-response curve showing Substance P activates Substance P-sniffer cells at low nanomolar concentrations (grey, EC_{50}=11.8 nM). 4-parameter variable slope dose-response curves were fit by non-linear regression. At least three replicates were performed for each concentration per condition, in two independent experiments.

139 ## 2.2. Loss of Substance P and CGRPα does not affect acute pain or itch

140 To understand whether neuropeptide signaling is required for pain sensation, we performed a
141 comprehensive battery of somatosensory behavior tests on DKO and wild-type control mice (WT).
142 Notably, regardless of the type of mechanical or thermal stimulus, groups of animals showed no
143 difference in their behavior (Figure 2). Specifically, responses to mechanical stimulation by von Frey
144 hairs, pinpricks or an alligator clip were quantitatively indistinguishable (Figure 2A-C). In addition,
145 withdrawal responses to radiant heat stimulation (Hargreaves', Figure 2D), and to two noxious Hot
146 Plate temperatures were unaffected in DKO mice (Figure 2E). Responses to cold evoked by acetone
147 and dry ice were also the same between groups (Figure 2F-G). Intraplantar injection of the Trpv1
148 agonist capsaicin evoked coping-like licking responses in both genotypes, however responses were
149 variable and although decreased licking was observed in some DKO mice, differences did not reach
150 statistical significance (Figure 2H). Therefore, to explore this potential difference using an
151 independent measure, we quantified capsaicin-evoked Fos staining as a correlate of dorsal horn
152 network activation. No differences in dorsal horn Fos expression were observed (Figure 2 – figure
153 supplement 1A-B). Furthermore, intraplantar injection of a different algogen (the Trpa1 agonist allyl
154 isothiocyanate, AITC) evoked similar licking behavior to capsaicin that was unaffected by peptide
155 deletion (Figure 2I). Together these data suggest that loss of the two neuropeptides does not alter
156 acute withdrawal or coping-like responses to multiple modalities of damaging stimuli applied to the
157 paw.

158 We investigated whether dual peptide deletion might attenuate visceral pain. First, we dosed
159 mice with acetic acid via intraperitoneal injection. This evoked comparable writhing behavior in both
160 WT and DKO mice (Figure 2J). Next, because NKR1 antagonists are effective anti-emetics, we
161 wondered whether the two peptides contribute to nausea-like behavior in mice (Warr et al., 2005). In
162 many species, lithium chloride induces gastrointestinal malaise and when paired with a normally
163 attractive tastant produces a marked conditioned taste aversion (Garcia et al., 1955). Notably, pairing
164 saccharin with LiCl injection elicited a strong and indistinguishable conditioned taste aversion in
165 both WT and DKO mice (Figure 2 – figure supplement 2A).

166 NKR1 antagonists have also been proposed to treat itch (Pojawa-Gołąb et al., 2019).
167 Therefore, we examined whether peptide deletion abrogated itching. DKO mice scratched robustly
168 following intradermal chloroquine injection, a response indistinguishable from WT animals (Figure

169 2K). Thus, our data demonstrate that Substance P and CGRPα contribute little to defensive
170 behaviors evoked by diverse sensory stimuli.

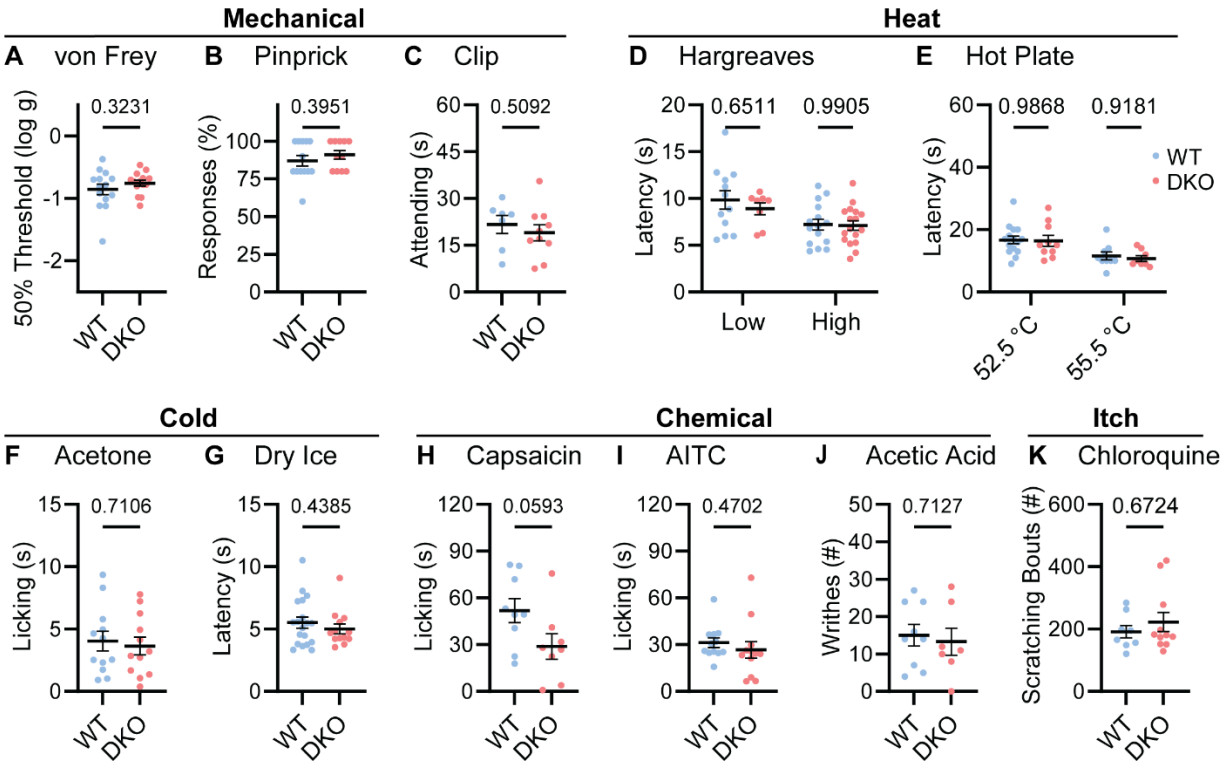

Figure 2. Tac1::Calca DKO mice respond to acute painful and itching stimuli. (**A)** 50% withdrawal threshold for von Frey punctate stimulation (log g). *n*=14 (7M, 7F) for WT & *n*=14 (7M, 7F) for DKO. (**B)** Percentage response to noxious pinprick stimulation. *n*=13 (5M, 8F) for WT & *n*=11 (4M, 7F) for DKO. **(C)** Time spent attending to alligator clip applied to paw for 60 s. *n*=7 (3M, 4F) for WT & *n*=10 (6M, 4F) for DKO. **(D)** Latency to withdraw to low and high radiant heat. For low setting, *n*=12 (6M, 6F) for WT & *n*=8 (4M, 4F) for DKO. For high setting, *n*=15 (8M, 7F) for WT & *n*=17 (9M, 8F) for DKO. **(E)** Latency to lick hindpaw following exposure to hot plate at two different temperatures. For 52.5 °C, *n*=15 (7M, 8F) for WT & *n*=10 (6M, 4F) for DKO. For 55.5 °C, *n*=9 (6M, 3F) for WT & *n*=8 (5M, 3F) for DKO. **(F)** Time spent licking in 60 s immediately following acetone application to paw. *n*=12 (5M, 7F) for WT & *n*=12 (5M, 7F) for DKO. (**D)** Latency to respond to dry ice. *n*=19 (8M, 11F) for WT & *n*=13 (5M, 8F) for DKO. (**H)** Time spent licking in 5 mins after capsaicin injection to paw. *n*=9 (4M, 5F) for WT & *n*=8 (4M, 4F) for DKO. (**I)** Time spent licking in 5 mins after 1% AITC injection to paw. *n*=12 (6M, 6F) for WT & *n*=12 (6M, 6F) for DKO. (**J)** Number of writhes in 15 mins starting 5 mins after intraperitoneal injection of 0.6% acetic acid. *n*=9 (5M, 4F) for WT & *n*=7 (5M, 2F) for DKO. (**K)** Scratching bouts in 15 minutes evoked by chloroquine injection into the nape of the neck. *n*=8 for WT & *n*=11 for DKO. For (A-C) and (F-K), means were compared using unpaired *t*-test, and for (D-E) a 2-Way ANOVA followed by post-hoc Sidak's test was used. Error bars denote standard error of the mean.

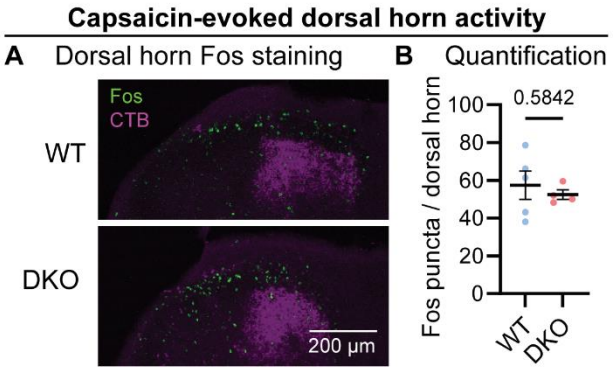

Figure 2 – figure supplement 1. Capsaicin evokes Fos activity in the dorsal horn of Tac1::Calca DKO mice. (A) Example confocal images showing dorsal horn of WT and DKO mice backlabelled with CTB (*magenta*) from the paw. Similar numbers of Fos puncta (*green*) are visible in the ipsilateral superficial dorsal horn of the WT and DKO cases. **(B)** Quantification of the mean number of Fos puncta in the ipsilateral dorsal horn of WT and DKO mice. For each mouse, the number of Fos puncta was counted in the 5 sections with the strongest CTB labelling and then averaged so that *n* is the number of mice. *n*=5 (2M, 3F) for WT & *n*=4 (2M, 2F) for DKO. Means were compared for (B) using an unpaired t test. Error bars denote standard error of the mean.

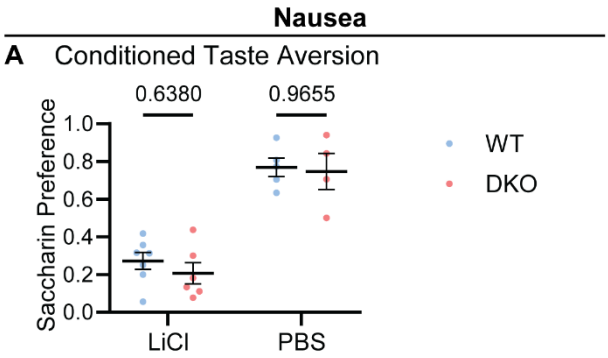

Figure 2 – figure supplement 2. Tac1::Calca DKO mice develop LiCl-induced conditioned taste aversion (A) Quantification of conditioned taste aversion (CTA) test in WT (blue) and DKO (red) mice. Saccharin preference index on test day is shown for animals given either lithium chloride or PBS following saccharin exposure on the conditioning day. Both WT and DKO treated with LiCl show a pronounced aversion to the usually-preferred saccharin. For LiCl, *n*=7 (4M, 3F) for WT & *n*=6 (4M, 2F) for DKO. For PBS, *n*=5 (3M, 2F) for WT & *n*=4 (2M, 2F) for DKO. Means were compared by 2-way ANOVA followed by post-hoc Sidak's test. Error bars denote standard error of the mean.

208

209 **2.3. Inflammatory pain and neurogenic inflammation are preserved in**
210 **Substance P and CGRPα-deficient mice**

211 Chronic inflammatory pain results in long lasting changes in nociceptor function and the
212 downstream pathways they engage. This plasticity is widely thought to involve neuropeptides
213 (Zieglgänsberger, 2019). We therefore tested whether loss of Substance P and CGRPα impacted the
214 development of heat hypersensitivity following treatment with Complete Freund's Adjuvant (CFA).
215 Surprisingly, WT and DKO mice with intraplantar injection of CFA developed strong heat
216 hypersensitivity (Figure 3A). Mechanical hypersensitivity was also unaffected by peptide loss (Figure
217 3B). CFA injection causes a long-term inflammatory immune response, therefore we also tested
218 Prostaglandin E2 (PGE2), which can acutely sensitize nociceptors. PGE2 injection elicited short-
219 lasting heat and mechanical hypersensitivity to a similar extent in both WT and DKO mice (Figure
220 3C-D). Together, these data indicate that Substance P and CGRPα are not required for the
221 behavioral sensitization associated with both acute and chronic inflammation.

222 Release of vasoactive peptides including Substance P and CGRPα from nociceptor terminals
223 has been proposed to drive neurogenic inflammation, encompassing oedema and extravasation
224 (Chiu et al., 2012). Unexpectedly, we noticed that injection of the inflammatory mediators CFA and
225 PGE2, as well as the algogens AITC and capsaicin, provoked swelling of the hindpaw of DKO mice
226 to a similar extent as WT mice. To examine the development of neurogenic inflammation more
227 rigorously, we measured paw volumes after capsaicin injection, and observed no appreciable
228 differences in capsaicin-induced swelling between WT and DKO mice. (Figure 3E-F). In addition,
229 using the Evans blue dye method, we found that plasma extravasation was intact in DKO mice
230 (Figure 3G). Similar results were observed following AITC injection (Figure 3H-J). Therefore,
231 Substance P and CGRPα are dispensable for some forms of neurogenic inflammation.

232

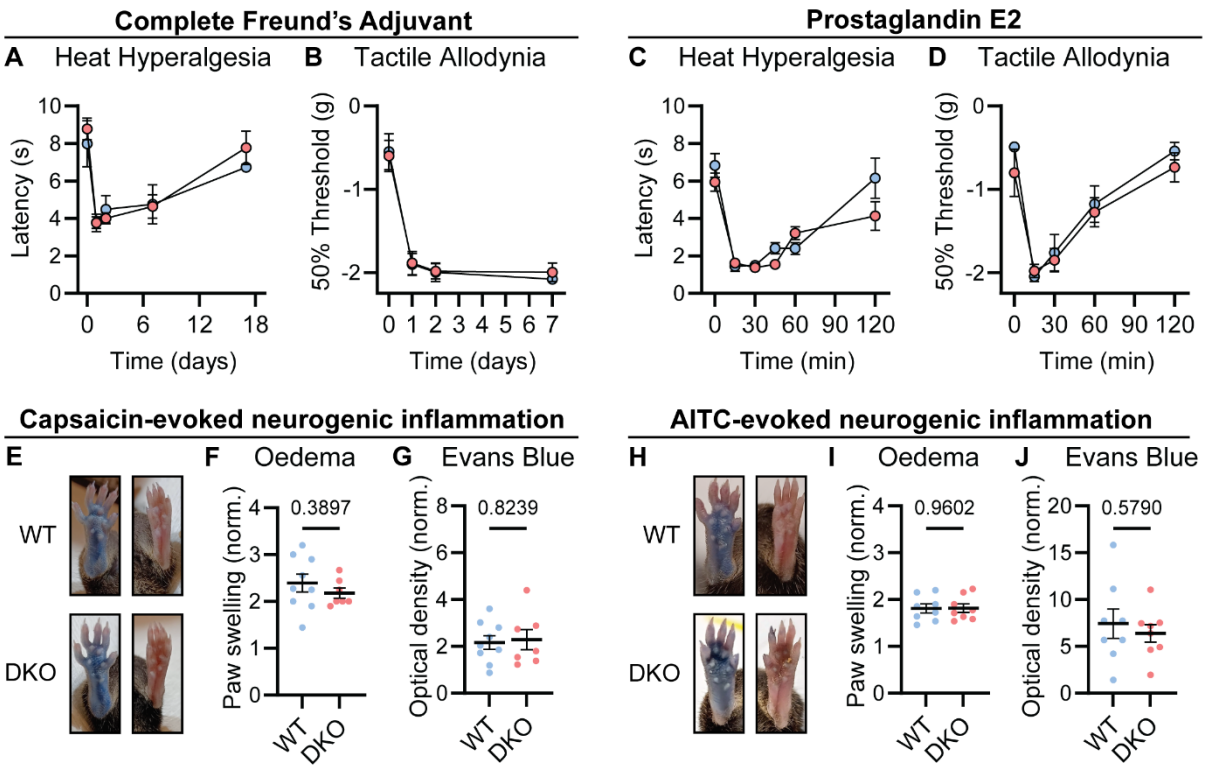

Figure 4. Tac1::Calca DKO mice display inflammatory pain and neurogenic inflammation. (A) Time course of the change in the Hargreaves' radiant heat withdrawal latencies of the hindpaw of WT and DKO mice following intraplantar injection of Complete Freund's Adjuvant (CFA). *n*=5 (5F) for WT & *n*=7 (2M, 5F) for DKO. **(B)** Time course of the change in von Frey 50% withdrawal thresholds (log g) on the hindpaw of WT and DKO mice after CFA. *n*=6 (3M, 3F) for WT & *n*=6 (3M, 3F) for DKO. **(C)** Time course of the change in the Hargreaves' radiant heat withdrawal latencies of the hindpaw of WT and DKO mice following intraplantar injection of Prostaglandin E2 (PGE2). *n*=10 (8M, 2F) for WT & *n*=10 (7M, 3F) for DKO. **(D)** Time course of the change in von Frey 50% withdrawal thresholds (log g) on the hindpaw of WT and DKO mice after PGE2. *n*=6 (3M, 3F) for WT & *n*=8 (3M, 3F) for DKO. **(E)** Images showing both WT and DKO mice show paw swelling and plasma extravasation following capsaicin injection (*left*) compared to uninjected paw (*right*). **(I)** Capsaicin-induced oedema, with injected paw swelling measured by volume and normalized to the uninjected paw, in WT and DKO mice. *n*=9 for WT (5M, 4F) & *n*=7 for DKO (4M, 3F). **(F)** Optical density of Evans blue dye extracted from the capsaicin-injected paw, normalized to uninjected paw, in WT and DKO mice. *n*=9 for WT (5M, 4F) & *n*=7 for DKO (4M, 3F). **(H)** Images showing both WT and DKO mice show paw swelling and plasma extravasation following AITC injection (*left*) compared to uninjected paw (*right*). **(I)** AITC-induced oedema, with injected paw swelling measured by volume and normalized to the uninjected paw, in WT and DKO mice. *n*=8 for WT (4M, 4F) & *n*=8 for DKO (4M, 4F). **(F)** Optical density of Evans blue dye extracted from AITC-injected paw, normalized to uninjected paw, in WT and DKO mice. *n*=8 for) & *n*=6 for DKO (4M, 4F). For (A-D), means were compared using 2-way ANOVA followed by post-hoc Sidak's test, and for (F-G) and (I-J), an unpaired *t*-test was used. Error bars denote standard error of the mean.

258 ## 2.4. Neuropathic pain is unaffected by Substance P and CGRPα deletion

259 Lastly, we investigated how dual peptide deletion affected the development of allodynia symptoms,
260 where innocuous stimuli are perceived as painful, in two mouse models of neuropathic pain (Jensen
261 and Finnerup, 2014). First, we performed a sciatic spared nerve injury on DKO animals and found
262 that the static mechanical allodynia evoked by von Frey filaments developed to the same degree as in
263 WT mice, persisting for several weeks (Figure 4A). Brush-evoked Fos activity in the superficial
264 laminae of the dorsal horn of SNI-treated mice – a correlate of dynamic allodynia – was also
265 comparable between genotypes (Figure 4B-C). Second, we treated mice with the chemotherapeutic
266 drug oxaliplatin which evokes extreme cold allodynia that is known to depend, in part, on CGRPα-
267 positive silent cold-sensing neurons (MacDonald et al., 2021). One day after intraplantar oxaliplatin
268 treatment, both DKO and WT animals displayed pronounced pain-like behaviors when placed on a
269 Cold Plate held at 10 °C (Figure 4D). Substance P and CGRPα are therefore not essential for
270 mechanical or cold allodynia.

271

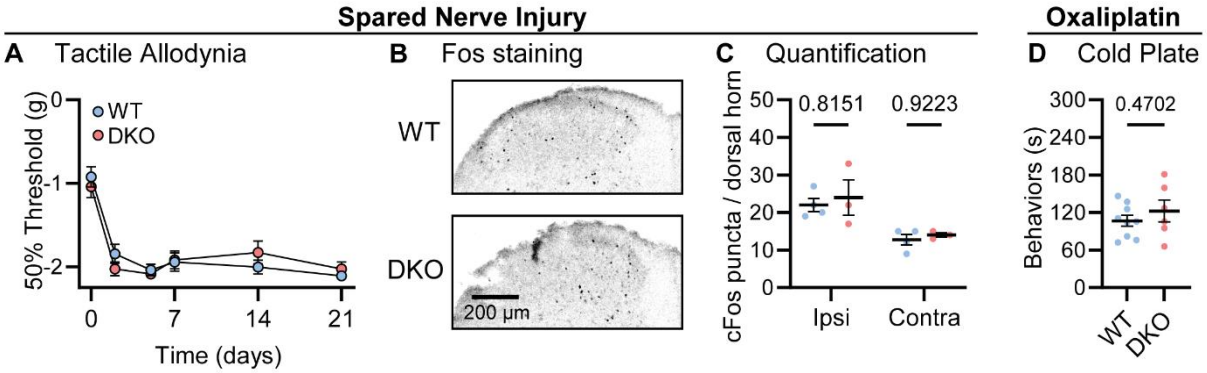

Figure 4. Tac1::Calca DKO mice develop neuropathic pain associated with nerve injury and the chemotherapeutic drug oxaliplatin. (A) Time course of the change in the von Frey 50% withdrawal threshold (log g) of the hindpaw of WT and DKO mice after sciatic spared nerve injury. *n*=8 (4M, 4F) for WT & *n*=8 (4M, 4F) for DKO. **(B)** Example confocal images showing Fos staining in the dorsal horn of WT and DKO mice following prolonged brushing of the lateral part of the plantar surface of the hindpaw ipsilateral to the spared nerve injured. More Fos puncta are visible in the ipsilateral compared to the contralateral dorsal horn of both WT and DKO cases. **(C)** Quantification of the mean number of Fos puncta in the ipsilateral and contralateral dorsal horn of WT and DKO mice. For each mouse, the number of Fos puncta was counted in 5 sections and then averaged so that *n* is the number of mice. *n*=4 for WT & *n*=3 for DKO. **(D)** Quantification of the time WT and DKO mice pre-treated with oxaliplatin (40 µg / 40 µl intraplantar) spent exhibiting pain-like behaviors in 5 minutes of exposure to a cold plate held at -10 °C. *n*=9 (5M, 4F) for WT & *n*=6 (3M, 3F) for DKO. Means were compared for (A) with a 2-Way ANOVA followed by post-hoc Sidak's test, and for (D) with an unpaired t test. Error bars denote standard error of the mean.

287 # 3. Discussion

288 The neuropeptides Substance P and CGRPα have been proposed to play diverse but largely
289 overlapping roles in acute, inflammatory and neuropathic pain. However, when the levels of peptide
290 signaling have been experimentally manipulated, effects have often been small and variable between
291 studies, possibly due to redundancy (Hohmann et al., 2004). We therefore generated DKO mice
292 lacking both Substance P and CGRPα signaling. Remarkably, both peptides were dispensable for
293 pain across a wide range of assays.

294 It is difficult to reconcile our findings with the fact that Substance P and CGRPα are highly
295 expressed throughout ascending pain pathways and are often found together in the same cells (Pauli
296 et al., 2022; Sharma et al., 2020; Zeisel et al., 2018). Studies of *Tac1* and *Calca* single KO mice
297 reported significant impairments in acute pain, including heat sensitivity, visceral pain and the
298 formalin test (Cao et al., 1998; Salmon et al., 2001, 1999; Zimmer et al., 1998). Notably, these deficits
299 were modest, and in fact inconsistent between studies (Woolf et al., 1998; Zajdel et al., 2021).
300 Nonetheless, ablating or inhibiting either peripheral or central neurons expressing Substance P and
301 CGRPα produces profound analgesia (Barik et al., 2018; Cowie et al., 2018; Han et al., 2015; McCoy
302 et al., 2013). Importantly, these neurons are all glutamatergic, and are thought to co-release
303 neuropeptides to modulate synaptic transmission and neuronal firing (Pagani et al., 2019). Our work
304 thus substantiates previous findings that established primary afferent-derived glutamate as the
305 critical transmitter for most pain sensations (Lagerström et al., 2011, 2010; Liu et al., 2010; Rogoz et
306 al., 2012; Scherrer et al., 2010), and suggests that the two peptides play at most a minor role.

307 An oft proposed caveat is that constitutive deletion of genes could be compensated for by
308 upregulating the expression of functionally similar molecules, but with surprisingly little evidence
309 (El-Brolosy and Stainier, 2017). Alternatively, neuropeptides may have opposing effects in different
310 parts of the circuitry meaning global loss of the gene may produce a net effect of no change in a
311 particular behavior. Indeed, classical studies show Substance P infusion into the spinal cord elicits
312 pain, but paradoxically in the brain is analgesic (Hylden and Wilcox, 1981; Malick and Goldstein,
313 1978). Despite this, knockout of a gene remains the strongest test of whether the molecule it
314 encodes is essential for a biological phenomenon (Caterina et al., 2000; Chesler et al., 2016; Mishra
315 and Hoon, 2013), and our results clearly demonstrate that Substance P and CGRPα are not required
316 for pain transmission.

317 The striking and highly-conserved pattern of expression of these two peptides in pain
318 pathways, particularly in nociceptors, raises the question of why these neurons evolved to release
319 them. Rather than directly acting as pain transmitters in the CNS, accumulating evidence indicates
320 the secretion of these neuropeptides from nociceptor peripheral terminals modulates immune cells
321 and the vasculature in diverse tissues. We focused on pain transmission, but it is clear our DKO
322 mice will be useful reagents for exploring the crosstalk between nociceptors and other body systems.
323 For example, the development of effective migraine therapeutics targeting CGRPα or its receptor
324 confirm the important role this peptide plays in headache (De Matteis et al., 2020; Tso and Goadsby,
325 2017), and new efferent functions for both CGRPα and Substance P are regularly being uncovered
326 (Brain, 1997; Caceres et al., 2009; Perner et al., 2020; Pinho-Ribeiro et al., 2016; Wilhelms et al.,
327 2018; Yang et al., 2022).

328 Beyond Substance P and CGRPα, pain-responsive neurons express a rich repertoire of
329 potential signaling molecules, including other neuropeptides. Emerging approaches to image and
330 manipulate these molecules (Girven et al., 2022; Kim et al., 2023), as well as advances in quantitating
331 pain behaviors (Bohic et al., 2023; MacDonald and Chesler, 2023), may ultimately reveal the
332 fundamental roles of neuropeptides in generating our experience of pain.

333

334

335

336 # 4. Acknowledgements

337 We are grateful to Nick Ryba for help and advice, and members of the Chesler lab for feedback.
338 This research was supported by the Intramural Research Program of the NIH, the National Center
339 for Complementary and Integrative Health, and the National Institute of Neurological Disorders
340 and Stroke (A.T.C.), a European Molecular Biology Organization Postdoctoral Fellowship (D.I.M.),
341 and a Branco Weiss Fellowship (D.I.M.).

342

343 # 5. Declaration of interests

344 The authors declare no conflict of interests.

345

346

347

348

349

350

351

6. Materials and Methods

6.1. Animals

Animal care and experimental procedures were performed in accordance with a protocol approved by the National Institute for Neurological Diseases and Stroke (NINDS) Animal Care and Use Committee. DKO mice were generated by crossing B6.Cg-Calcatm1.1(cre/EGFP)Rpa/J (Jax #033168) with Tac1-tagRFP-2A-TVA (Carter et al., 2013; Wu et al., 2018). Both male and female (> 6 weeks) mice were used for all experiments, and the number of mice of each sex used to generate each dataset is reported in the legend. The experimenters were blinded to genotype throughout. Genomic DNA was isolated from tail biopsy for genotyping by Transnetyx.

6.2. Immunohistochemistry

6.2.1. Substance P and CGRPα staining

Mice were anesthetized with isoflurane and perfused intracardially with heparin then 4% PFA. Tissue was post-fixed in 4% PFA overnight and then cryoprotected in 30% sucrose. Tissue was mounted in OCT and cut using a cryostat into 40-50 micron sections. The sections were incubated in a blocking buffer (5% donkey serum; 0.1% Triton X-100; PBS) for 3 hours at room temperature on a shaker. The sections were incubated in 1:500 goat anti-CGRP polyclonal primary antibody (Abcam, #ab36001) or 1:500 rabbit anti substance P polyclonal primary antibody (Abcam, #ab67006) at room temperature overnight. The sections were rinsed 2 times with PBS and then incubated for 2 hours in 1:200 Cy5-conjugated donkey anti-rabbit secondary antibody or 1:200 Cy5-conjugated donkey anti-goat secondary antibody (Thermo Fisher Scientific). The sections were rinsed 2 times with PBS and mounted in ProLong diamond antifade mounting media (Thermo Fisher Scientific) onto slides (Daigger Scientific). Z-stacks were acquired on an Olympus confocal microscope using a 20x objective and processed using ImageJ/FIJI software (National Institute of Health).

6.2.2. Fos staining for neuronal activity

Mice were injected with 10 microliters of 0.1% Alexa Fluor 647 conjugated cholera toxin subunit B into one hindpaw so that the spinal cord sections innervating the paw could later be identified. After 1 week, mice were habituated then the stimulation was performed. For capsaicin-evoked dorsal horn

380 Fos, capsaicin (0.3%) was injected into the right hindpaw of mice in chambers on a plexiglass stand.
381 For Fos elicited by dynamic allodynia stimulation, mice that received a spared nerve injury procedure
382 3 weeks prior were stimulated with a paint brush while housed on a wire mesh stand (3 x 10 min
383 stimulation period, with 1 minute rest every 10 mins). Note that for SNI experiments, the CTB was
384 injected into the contralateral paw, because severing two branches of the sciatic nerve prevents
385 efficient CTB transit in the ipsilateral paw. The mice were perfused as above and spinal cords were
386 harvested 75-120 mins after stimulation. The sections were incubated in a blocking buffer (5% goat
387 serum; 0.1% Triton X-100; PBS) for 3 hours at room temperature on a shaker. The sections were
388 incubated in 1:1000 rabbit anti Fos primary antibody (Cell Signaling Technology, Phospho-c-Fos
389 (Ser32) (D82C12) XP® Rabbit mAb, #5348) at room temperature overnight. The sections were
390 rinsed 2 times with PBS and incubated for 2 hours in 1:5000 Alexa Fluor 750 goat anti-rabbit
391 secondary antibody (Life Technologies). The sections were rinsed 2 times with PBS and mounted in
392 ProLong diamond antifade mounting media (Thermo Fisher Scientific) onto slides (Daigger
393 Scientific). Z-stack images were acquired on an Olympus confocal microscope using a 20x objective.
394 The five sections with the greatest Alexa Fluor 647 cholera toxin subunit B signal were imaged for
395 each mouse. This ensured Fos activity was measured only in those sections strongly innervated by
396 the hindpaw. The number of Fos positive nuclei in the dorsal horn were quantified in ImageJ/FIJI
397 software (National Institute of Health) by a blinded observer using a semi-automated procedure.
398 The counts for the five sections were averaged for each mouse.

399

400 6.3. Neuropeptide Imaging

401 6.3.1. Generation and maintenance of Substance P-sniffer cell line

402 To generate the Substance P-sniffer cell line, we produced a mouse *Tacr1* DNA construct by gene
403 synthesis (Epoch Life Science, GS66243-3). *Tacr1* was subcloned along with a synthesized human G-
404 protein α-subunit gene Gα15 and *GCaMP6s* it into the lentiviral plasmid backbone pLV-CMV-
405 PGK-Hyg (Cellomics Technology, LVR-1046) to create the final lentiviral plasmid pLV-CMV-
406 GCaMP6s-P2A-TACR1-T2A-hG15-PGK-Hyg. We used this plasmid to produce lentiviral particles
407 (Vigene Biosciences) and infected them into human embryonic kidney cells at a multiplicity of
408 infection of 20 following manufacturer's instructions. The Flp-In T-REx HEK293 cell line was used

409 (Thermo Fisher Scientific, R78007). Stably expressing cells were isolated by treating with 200 μg/mL
410 hygromycin B (Thermo Fisher Scientific, 10687010).

411 The cell lines were maintained on polystyrene culture plates (Fisher Scientific, 07-200-80) in a 5%
412 CO_2 humidified incubator at 37°C. The growth medium was changed every 2–3 days and consisted
413 of DMEM/F12 (Fisher Scientific, 11330032) supplemented with 10% fetal bovine serum (Fisher
414 Scientific, 26140079) and 200 μg/mL hygromycin B. Cells were passaged when they reached
415 confluency, which was roughly twice per week, and were never propagated past 20 passages. For
416 passaging, cells were rinsed in PBS (Fisher Scientific, 10010023) and then incubated in Accutase
417 (Fisher Scientific, 00-4555-56) for ~5 min at 37°C to detach. Cells were collected in a 15 mL tube
418 (Fisher Scientific, 12-565-268) and centrifuged at 300 rcf for 3 min to pellet. The supernatant was
419 aspirated, and cells were resuspended in growth medium followed by plating in new polystyrene
420 plates. Typical dilution ratios for passaging were between 1:3 and 1:20. For imaging, Substance P-
421 sniffer cells were cultured onto 8-chamber glass slides, and imaged before they reached confluency.

422 **6.3.2. Adult dorsal root ganglion culture and Substance P-sniffer co-culture**

423 Dorsal root ganglia (DRG) were dissected from the entire length of the spinal column and then
424 digested in a pre-equilibrated enzyme mix for 35-45 minutes (37 °C, 5% CO2). The enzyme mix
425 consisted of Hanks' balanced salt solution containing collagenase (type XI; 5 mg/ml), dispase (10
426 mg/ml), HEPES (5 mM) and glucose (10 mM). DRGs were then gently centrifuged for 3 minutes at
427 300 revolutions per minute, the supernatant was discarded and replaced with warmed DMEM/F-12,
428 supplemented with 10% fetal bovine serum (FBS). Next, DRGs were mechanically triturated with
429 three fire-polished glass Pasteur pipettes of gradually decreasing inner diameter. Dissociated cells
430 were then centrifuged again at 300 revolutions per minute, the supernatant was discarded and cells
431 were re-suspended in the required volume of DMEM supplemented with FBS and nerve growth
432 factor (50 ng/ml). Finally, cells were plated onto 8-chamber glass slides coated with poly-L-lysine (1
433 mg/ml) and laminin (1 mg/ml), and incubated at 37 °C in 5% CO2. 24 hours later, Substance P-
434 sniffer cells were resuspended in DMEM/F-12, supplemented with 10% fetal bovine serum (FBS)
435 and nerve growth factor (50 ng/ml). 70,000 cells were dispensed into each imaging chamber
436 containing DRG neurons, and incubated for at least a further 24 hours before imaging was
437 performed.

438 **6.3.3. In vitro imaging**

439 Imaging was performed in Ringer's solution: 125 mM NaCl, 3 mM KCl, 5 mM $CaCl_2$, 1 mM $MgCl_2$,
440 10 mM glucose, and 10 mM HEPES (all from Sigma-Aldrich), adjusted to pH 7.3 with 1 M NaOH,
441 and osmolality measured ~280 mmol/kg. SP-sniffer cells alone, or co-cultured with DRGs, were
442 rinsed in Ringer's solution and imaged in Ringer's solution at room temperature on an Olympus
443 IX73 inverted microscope using a pco.panda sCMOS back-illuminated camera at 2 frames per
444 second. Tac1-RFP was excited at 560 nm LED and GCaMP6f at 488 nm. All imaging trials began
445 with 15 s of baseline measurement and then the cells were treated with chemicals by micropipette.
446 The chemicals used were capsaicin (10 μM) and Substance P amide (1 pM to 1μM). The peak $\Delta F/F_0$
447 was calculated to quantify the changes in fluorescence associated with chemical application, with F_0
448 defined as the mean fluorescence intensity of the entire field of view in the 5 s immediately
449 preceding stimulation.

450

451 ## 6.4. Behavioral Assays

452 ### 6.4.1. Von Frey

453 Punctate mechanical sensitivity was measured using the up-down method of Chaplan to obtain a
454 50% withdrawal threshold (Chaplan et al., 1994). Mice were habituated on a mesh wire stand for 1
455 hour. A 0.16g Von Frey hair was applied to the plantar region of the paw for 2 s. A response was
456 recorded when the mouse swiftly lifted its paw in response to the stimulus. A positive response
457 resulted in application of a filament of lesser strength on the following trial, and no response in
458 application of a stronger filament. To calculate the 50% withdrawal threshold, five responses
459 surrounding the 50% threshold were obtained after the first change in response. The pattern of
460 responses was used to calculate the 50% threshold = $(10[\chi+\varkappa\delta])/10{,}000)$, where χ is the log of the
461 final von Frey filament used, $\varkappa$ = tabular value for the pattern of responses and δ the mean
462 difference between filaments used in log units. The log of the 50% threshold was used to calculate
463 summary and test statistics.

464 ### 6.4.2. Pinprick

465 Mice were habituated on a mesh wire stand for 1 hour. A 27-gauge needle was blunted and used to
466 apply pressure to the hind paw. A withdrawal response was quantified as the mouse lifting the paw
467 swiftly away from the blunted needle. The pinprick stimulation was repeated for 5 or 10 trials with
468 5-minute breaks inbetween. The percentage of withdrawal responses was calculated for each mouse.

469 **6.4.3. Clip**

470 Mice were habituated in opaque chambers on a plexiglass stand for 1 hour. The mouse was
471 restrained and an alligator clip was applied to the hindpaw just in front of the heel. The mouse was
472 returned to the chamber. The mouse's behavioral response was recorded from below using a video
473 camera. After 60 s, the clip was removed. The amount of time the mouse spent attending the clip
474 and associated paw was quantified post-hoc by a blinded observer. Attending was defined as
475 biting/handling the clip, and biting/licking the paw.

476 **6.4.4. Hargreaves**

477 Mice were habituated on a plexiglass stand for 1 hour with the Hargreaves machine turned on in a
478 dark room. The radiant heat stimulus was aimed for the centre of the plantar region of the mouse's
479 hind paw. The response latency was recorded for 5 trials with 10-minute breaks in between each
480 trial.

481 **6.4.5. Hot/Cold Plate**

482 The plate was set to the desired temperature. A camera set up with a mirror was used for better
483 visibility of the mouse on the hot plate. A clear cylindrical tube was placed around the hot plate to
484 ensure the mouse cannot escape. Once the hot plate reached the set temperature, the mouse was
485 placed on the hot plate and the top of the cylinder was covered. At the cut-off time, the mouse was
486 taken off the hot plate and placed back in the cage. The latency to lick was scored post-hoc using the
487 recorded videos by a blinded observer.

488 **6.4.6. Dry Ice**

489 Mice were habituated on a plexiglass floor stand for 1 hour. A 2 ml plastic syringe was cut in half to
490 allow for crushed dry ice to be compacted into the tube. The dry ice was pushed up against the glass
491 where the mouse's hind paw was resting. Withdrawal latency was recorded with a stopwatch. 10
492 minutes were given in between each trial. The procedure was repeated 5 times and an average of the
493 withdrawal latencies was calculated.

494 **6.4.7. Acetone**

495 Mice were habituated on a plexiglass floor stand for 1 hour. Mice were videotaped as acetone was
496 applied to the plantar region of their hind paw. Behavior was scored post-hoc by a blinded
497 observer and the total amount of time spent licking the paw in a 60 second time interval was
498 recorded. The experiment was repeated for a second trial and average scores were used.

499 **6.4.8. Chemical Algogens**

500 Mice were habituated on a plexiglass stand for 1 hour. 0.3 mM capsaicin in 90% saline / 10%
501 Tween-20 / 1% ethanol or 1% AITC in saline was injected into the plantar surface of the hind paw.
502 Mice were video-taped for 5 minutes. A blinded observer scored the amount of time in seconds the
503 mouse spent licking the injected paw in a 5-minute time period.

504 **6.4.9. Acetic Acid**

505 Mice were habituated on a plexiglass stand for 1 hour. 0.6% of acetic acid was injected
506 intraperitoneally at a dose of 10 µl per gram weight of the animal. Mice were videotaped for 20
507 minutes. The number of writhes was quantified post-hoc by a blinded observer during a 15-minute
508 interval between 5 and 20 minutes after injection.

509 **6.4.10. Conditioned Taste Aversion**

510 Mice were single-housed and habituated for 3 days to drink from two glass bottles with stainless-
511 steel ball-bearing spouts. Mice then received 3 days of training, where they were water-deprived for
512 22 hours followed by 30 mins exposure to a single water-containing bottle, then 90 mins exposure to
513 both bottles. On the conditioning day, after 22 hours of water deprivation, mice were exposed to a
514 single bottle containing saccharin water (15 mM) for 45 mins. Mice were then injected with lithium
515 chloride (200 mg/kg) or PBS, and then given ordinary water for 75 mins. The animals were then
516 water deprived for a further 22 hours. On the test day, mice were simultaneously exposed to a bottle
517 containing water and a bottle containing saccharin for 45 mins. The volume of each solution
518 consumed was measured by weighing the bottles before and after. To calculate the saccharin
519 preference index of each animal, the volume of saccharin consumed was divided by the total of fluid
520 consumed, with a value less than 0.5 indicating the development of an aversion to saccharin.

521 **6.4.11. Chloroquine-induced itch**

522 Hair from the nape of the mouse's neck was removed 2-3 days prior to behavioral experiments
523 using VEET hair removal cream and the area thoroughly washed and moisturizing cream applied.
524 Mice were habituated to transparent acrylic chambers (10cm x 10cm x 13cm) 30 minutes prior to
525 injection. Post habituation, a blinded investigator injected 20 µl of 25 µM Chloroquine diphosphate
526 salt (Sigma-Aldrich: C6628) solution in 0.9% saline intradermally into the nape of the neck using a
527 31G insulin syringe. Videos were quantified by a separate blinded investigator with a scratching bout
528 counted each time the mouse attended to the injected area with the hind paw after the paw was
529 removed from the floor or mouth.

530 **6.4.12. Inflammatory Pain Models**

531 CFA and PGE2 was purchased from Sigma. 20 µl of CFA was injected into the heel of the hind
532 paw. PGE2 (20 µl, 500 nM) was injected into the plantar surface of the hindpaw, and behavior was
533 assessed over the same time-frame that produces *in vivo* sensitization of nociceptor responses.
534 Inflammation-induced hypersensitivity was measured using the Hargreaves and the von Frey, as
535 described above.

536 **6.4.13. Spared Nerve Injury**

537 The mouse was anesthetized with isofluorane. The mouse was placed under the nose cone, belly
538 down, and the left hind limb area was shaved. The area was wiped clean with an ethanol wipe and
539 coated with betadine. Once the mouse was unresponsive, a 1-inch horizontal cut was made in the
540 skin right along the femur. Once the natural separation of muscles was located, a small scissor tool
541 was used to puncture the fascia and separate out the muscles. Once the sciatic nerve was located,
542 curved forceps were used to separate out the nerve from the muscle. The nerve was traced towards
543 the knee until the branch of three nerves (perineal, tibial and sural) was found. The sural nerve was
544 spared and the perineal and tibial nerves were cut. The mouse was sutured up and placed back in the
545 homecage for recovery without postoperative analgesics. Mechanical allodynia was assessed using
546 the von Frey assay as above.

547 **6.4.14. Oxaliplatin**

548 Chemotherapy-induced neuropathy was induced in mice by intraplantar injection of oxaliplatin into
549 the left hind paw (MacDonald et al., 2021). Oxaliplatin was made up to a dose of 80 µg in 40 µl of
550 5% glucose solution, due to its instability in chloride-containing saline solution. The number of
551 nocifensive behaviors in 5 mins was assessed on the Cold Plate held at 10 °C 24 hours later.

552 6.5. Neurogenic Inflammation

553 **6.5.1. Evans Blue assay**

554 Mice were anesthetized using isoflurane. 200 µl of Evans Blue dye was injected into the mouse's tail
555 vein. 15 mins later, one hindpaw was injected with an algogen. After a further 30 mins, the volume
556 of each paw was measured by displacement using a plethysmometer (Ugo Basile). Both paws were
557 then cut at the ankle and placed in tubes in the oven at 55 °C for 24 hours to dry. 1 ml of
558 formamide was then added to each paw and incubated for 4-6 days at 55 °C to extract the dye from
559 the paw tissue. 50 µl samples of dye-infused formamide from each paw were then dispensed to a 96

well plate in duplicate, along with a range of Evans blue dilutions in formamide to generate a standard curve. The optical density of each sample was then measured using a plate-reader, and the concentration of Evans Blue per paw sample interpolated from the standard curve to generate an index of extravasation in that paw.

6.6. Statistical Analysis

Data were compared using two-way ANOVA with post-hoc Sidak's test, or Student's t test. The α value was 0.05. For all experiments *n* is the number of animals, except Substance P imaging where *n* is the number of chambers. Error bars denote standard error of the mean throughout. No power analyses were used to determine sample sizes, but our sample sizes are similar to those from previous studies. Graphs were generated and statistical analysis was performed using GraphPad 8.0 software (Prism).

573 # 7. References

574 Amara SG, Jonas V, Rosenfeld MG, Ong ES, Evans RM. 1982. Alternative RNA processing in
575 calcitonin gene expression generates mRNAs encoding different polypeptide products. *Nature*
576 **298**:240–244. doi:10.1038/298240A0

577 Barik A, Thompson JH, Seltzer M, Ghitani N, Chesler AT. 2018. A Brainstem-Spinal Circuit
578 Controlling Nocifensive Behavior. *Neuron* **100**:1491-1503.e3. doi:10.1016/j.neuron.2018.10.037

579 Bohic M, Pattison LA, Jhumka ZA, Rossi H, Thackray JK, Ricci M, Mossazghi N, Foster W,
580 Ogundare S, Twomey CR, Hilton H, Arnold J, Tischfield MA, Yttri EA, St. John Smith E,
581 Abdus-Saboor I, Abraira VE. 2023. Mapping the neuroethological signatures of pain, analgesia,
582 and recovery in mice. *Neuron*. doi:10.1016/J.NEURON.2023.06.008

583 Brain SD. 1997. Sensory neuropeptides: their role in inflammation and wound healing.
584 *Immunopharmacology* **37**:133–152. doi:10.1016/S0162-3109(97)00055-6

585 Caceres AI, Brackmann M, Elia MD, Bessac BF, Del Camino D, D'Amours M, Witek JAS, Fanger
586 CM, Chong JA, Hayward NJ, Homer RJ, Cohn L, Huang X, Moran MM, Jordt SE. 2009. A
587 sensory neuronal ion channel essential for airway inflammation and hyperreactivity in asthma.
588 *Proc Natl Acad Sci U S A* **106**. doi:10.1073/pnas.0900591106

589 Cao YQ, Mantyh PW, Carlson EJ, Gillespie AM, Epstein CJ, Basbaum AI. 1998. Primary afferent
590 tachykinins are required to experience moderate to intense pain. *Nature 1998 392:6674*
591 **392**:390–394. doi:10.1038/32897

592 Carter ME, Soden ME, Zweifel LS, Palmiter RD. 2013. Genetic identification of a neural circuit that
593 suppresses appetite. *Nature 2013 503:7474* **503**:111–114. doi:10.1038/nature12596

594 Caterina MJ, Leffler A, Malmberg AB, Martin WJ, Trafton J, Petersen-Zeitz KR, Koltzenburg M,
595 Basbaum AI, Julius D. 2000. Impaired nociception and pain sensation in mice lacking the
596 capsaicin receptor. *Science* **288**:306–13.

597 Chaplan SR, Bach FW, Pogrel JW, Chung JM, Yaksh TL. 1994. Quantitative assessment of tactile
598 allodynia in the rat paw. *J Neurosci Methods* **53**:55–63.
599 Chen JY, Campos CA, Jarvie BC, Palmiter RD. 2018. Parabrachial CGRP Neurons Establish and
600 Sustain Aversive Taste Memories. *Neuron* **100**:891-899.e5.
601 doi:10.1016/J.NEURON.2018.09.032
602 Chesler A, Szczot M, Bharucha-Goebel D, Čeko M, Donkervoort S, Laubacher C, Hayes L, Alter K,
603 Zampieri C, Stanley C, Innes A, Mah J, Grosmann C, Bradley N, Nguyen D, Foley A, Le
604 Pichon C, Bönnemann C. 2016. The Role of PIEZO2 in Human Mechanosensation. *N Engl J*
605 *Med* **375**. doi:10.1056/NEJMOA1602812
606 Chiu IM, Von Hehn CA, Woolf CJ. 2012. Neurogenic inflammation and the peripheral nervous
607 system in host defense and immunopathology. *Nat Neurosci*. doi:10.1038/nn.3144
608 Cowie AM, Moehring F, O'Hara C, Stucky CL. 2018. Optogenetic Inhibition of CGRPα Sensory
609 Neurons Reveals Their Distinct Roles in Neuropathic and Incisional Pain. *J Neurosci* **38**:5807–
610 5825. doi:10.1523/JNEUROSCI.3565-17.2018
611 De Felipe C, Herrero JF, O'Brien JA, Palmer JA, Doyle CA, Smith AJH, Laird JMA, Belmonte C,
612 Cervero F, Hunt SP. 1998. Altered nociception, analgesia and aggression in mice lacking the
613 receptor for substance P. *Nature* **392**. doi:10.1038/32904
614 De Matteis E, Guglielmetti M, Ornello R, Spuntarelli V, Martelletti P, Sacco S. 2020. Targeting
615 CGRP for migraine treatment: mechanisms, antibodies, small molecules, perspectives.
616 *https://doi.org/101080/1473717520201772758* **20**:627–641.
617 doi:10.1080/14737175.2020.1772758
618 Drucker DJ. 2022. GLP-1 physiology informs the pharmacotherapy of obesity. *Mol Metab*.
619 doi:10.1016/j.molmet.2021.101351

620 El-Brolosy MA, Stainier DYR. 2017. Genetic compensation: A phenomenon in search of
621 mechanisms. *PLoS Genet*. doi:10.1371/journal.pgen.1006780
622 Garcia J, Kimeldorf DJ, Koelling RA. 1955. Conditioned Aversion to Saccharin Resulting from
623 Exposure to Gamma Radiation. *Science (1979)* **122**. doi:10.1126/science.122.3160.157
624 Girven KS, Mangieri L, Bruchas MR. 2022. Emerging approaches for decoding neuropeptide
625 transmission. *Trends Neurosci* **45**:899–912. doi:10.1016/j.tins.2022.09.005
626 Guo TZ, Wei T, Shi X, Li WW, Hou S, Wang L, Tsujikawa K, Rice KC, Cheng K, Clark DJ,
627 Kingery WS. 2012. Neuropeptide deficient mice have attenuated nociceptive, vascular, and
628 inflammatory changes in a tibia fracture model of complex regional pain syndrome. *Mol Pain* **8**.
629 doi:10.1186/1744-8069-8-85
630 Han S, Soleiman M, Soden M, Zweifel L, Palmiter RD. 2015. Elucidating an Affective Pain Circuit
631 that Creates a Threat Memory. *Cell* **162**:363–374. doi:10.1016/j.cell.2015.05.057
632 Hill R. 2000. NK1 (substance P) receptor antagonists - Why are they not analgesic in humans? *Trends*
633 *Pharmacol Sci* **21**:244–246. doi:10.1016/S0165-6147(00)01502-9
634 Hohmann JG, Teklemichael DN, Weinshenker D, Wynick D, Clifton DK, Steiner RA. 2004.
635 Obesity and Endocrine Dysfunction in Mice with Deletions of both Neuropeptide Y and
636 Galanin. *Mol Cell Biol* **24**. doi:10.1128/mcb.24.7.2978-2985.2004
637 Huang T, Lin SH, Malewicz NM, Zhang Yan, Zhang Ying, Goulding M, LaMotte RH, Ma Q. 2019.
638 Identifying the pathways required for coping behaviours associated with sustained pain. *Nature*
639 **565**:86–90. doi:10.1038/s41586-018-0793-8
640 Hylden JLK, Wilcox GL. 1981. Intrathecal substance P elicits a caudally-directed biting and
641 scratching behavior in mice. *Brain Res* **217**. doi:10.1016/0006-8993(81)90203-1
642 Jensen TS, Finnerup NB. 2014. Allodynia and hyperalgesia in neuropathic pain: clinical
643 manifestations and mechanisms. *Lancet Neurol* **13**:924–935. doi:10.1016/S1474-4422(14)70102-4

644 Jin Y, Smith C, Monteith D, Brown R, Camporeale A, McNearney TA, Deeg MA, Raddad E, Xiao
645 N, de la Peña A, Kivitz AJ, Schnitzer TJ. 2018. CGRP blockade by galcanezumab was not
646 associated with reductions in signs and symptoms of knee osteoarthritis in a randomized
647 clinical trial. *Osteoarthritis Cartilage* **26**:1609–1618. doi:10.1016/J.JOCA.2018.08.019
648 Kang SJ, Liu S, Ye M, Kim D Il, Pao GM, Copits BA, Roberts BZ, Lee KF, Bruchas MR, Han S.
649 2022. A central alarm system that gates multi-sensory innate threat cues to the amygdala. *Cell*
650 *Rep* **40**. doi:10.1016/j.celrep.2022.111222
651 Kim D-I, Park S, Ye M, Chen JY, Jhang J, Hunker AC, Zweifel LS, Palmiter RD, Han S. 2023.
652 Novel genetically encoded tools for imaging or silencing neuropeptide release from presynaptic
653 terminals in vivo. *bioRxiv* 2023.01.19.524797. doi:10.1101/2023.01.19.524797
654 Lagerström MC, Rogoz K, Abrahamsen B, Lind AL, Ölund C, Smith C, Mendez JA, Wallén-
655 Mackenzie Å, Wood JN, Kullander K. 2011. A sensory subpopulation depends on vesicular
656 glutamate transporter 2 for mechanical pain, and together with substance P, inflammatory pain.
657 *Proc Natl Acad Sci U S A* **108**:5789–5794. doi:10.1073/pnas.1013602108
658 Lagerström MC, Rogoz K, Abrahamsen B, Persson E, Reinius B, Nordenankar K, Ölund C, Smith
659 C, Mendez JA, Chen ZF, Wood JN, Wallén-Mackenzie Å, Kullander K. 2010. VGLUT2-
660 Dependent Sensory Neurons in the TRPV1 Population Regulate Pain and Itch. *Neuron* **68**.
661 doi:10.1016/j.neuron.2010.09.016
662 Latremoliere A, Woolf CJ. 2009. Central Sensitization: A Generator of Pain Hypersensitivity by
663 Central Neural Plasticity. *Journal of Pain*. doi:10.1016/j.jpain.2009.06.012
664 Lein ES, Hawrylycz MJ, Ao N, Ayres M, Bensinger A, Bernard A, Boe AF, Boguski MS, Brockway
665 KS, Byrnes EJ, Chen Lin, Chen Li, Chen TM, Chin MC, Chong J, Crook BE, Czaplinska A,
666 Dang CN, Datta S, Dee NR, Desaki AL, Desta T, Diep E, Dolbeare TA, Donelan MJ, Dong
667 HW, Dougherty JG, Duncan BJ, Ebbert AJ, Eichele G, Estin LK, Faber C, Facer BA, Fields R,

668 Fischer SR, Fliss TP, Frensley C, Gates SN, Glattfelder KJ, Halverson KR, Hart MR,
669 Hohmann JG, Howell MP, Jeung DP, Johnson RA, Karr PT, Kawal R, Kidney JM, Knapik
670 RH, Kuan CL, Lake JH, Laramee AR, Larsen KD, Lau C, Lemon TA, Liang AJ, Liu Y, Luong
671 LT, Michaels J, Morgan JJ, Morgan RJ, Mortrud MT, Mosqueda NF, Ng LL, Ng R, Orta GJ,
672 Overly CC, Pak TH, Parry SE, Pathak SD, Pearson OC, Puchalski RB, Riley ZL, Rockett HR,
673 Rowland SA, Royall JJ, Ruiz MJ, Sarno NR, Schaffnit K, Shapovalova N V., Sivisay T,
674 Slaughterbeck CR, Smith SC, Smith KA, Smith BI, Sodt AJ, Stewart NN, Stumpf KR, Sunkin
675 SM, Sutram M, Tam A, Teemer CD, Thaller C, Thompson CL, Varnam LR, Visel A, Whitlock
676 RM, Wohnoutka PE, Wolkey CK, Wong VY, Wood M, Yaylaoglu MB, Young RC,
677 Youngstrom BL, Yuan XF, Zhang B, Zwingman TA, Jones AR. 2007. Genome-wide atlas of
678 gene expression in the adult mouse brain. *Nature* **445**. doi:10.1038/nature05453
679 Liu Y, Abdel Samad O, Zhang L, Duan B, Tong Q, Lopes C, Ji RR, Lowell BB, Ma Q. 2010.
680 VGLUT2-Dependent Glutamate Release from Nociceptors Is Required to Sense Pain and
681 Suppress Itch. *Neuron* **68**:543–556. doi:10.1016/j.neuron.2010.09.008
682 Löken LS, Braz JM, Etlin A, Sadeghi M, Bernstein M, Jewell M, Steyert M, Kuhn J, Hamel K,
683 Llewellyn-Smith IJ, Basbaum A. 2021. Contribution of dorsal horn cgrp-expressing
684 interneurons to mechanical sensitivity. *Elife* **10**. doi:10.7554/eLife.59751
685 MacDonald DI, Chesler AT. 2023. Painspotting. *Neuron* **111**:2773–2774.
686 doi:10.1016/j.neuron.2023.08.026
687 MacDonald DI, Luiz AP, Iseppon F, Millet Q, Emery EC, Wood JN. 2021. Silent cold-sensing
688 neurons contribute to cold allodynia in neuropathic pain. *Brain*. doi:10.1093/brain/awab086
689 Malick JB, Goldstein JM. 1978. Analgesic activity of substance P following intracerebral
690 administration in rats. *Life Sci* **23**. doi:10.1016/0024-3205(78)90518-0

691 McCoy ES, Taylor-Blake B, Street SE, Pribisko AL, Zheng J, Zylka MJ. 2013. Peptidergic CGRPα
692 Primary Sensory Neurons Encode Heat and Itch and Tonically Suppress Sensitivity to Cold.
693 *Neuron* **78**. doi:10.1016/j.neuron.2013.01.030
694 Mishra SK, Hoon MA. 2013. The cells and circuitry for itch responses in mice. *Science (1979)* **340**.
695 doi:10.1126/science.1233765
696 Nahin RL, Feinberg T, Kapos FP, Terman GW. 2023. Estimated Rates of Incident and Persistent
697 Chronic Pain Among US Adults, 2019-2020. *JAMA Netw Open* **6**:e2313563.
698 doi:10.1001/JAMANETWORKOPEN.2023.13563
699 Nguyen MQ, von Buchholtz LJ, Reker AN, Ryba NJP, Davidson S. 2021. Single-nucleus
700 transcriptomic analysis of human dorsal root ganglion neurons. *Elife* **10**.
701 doi:10.7554/ELIFE.71752
702 Ogunlaja OI, Goadsby PJ. 2022. Headache: Treatment update. *eNeurologicalSci*.
703 doi:10.1016/j.ensci.2022.100420
704 Pagani M, Albisetti GW, Sivakumar N, Wildner H, Santello M, Johannssen HC, Ulrich H,
705 Correspondence Z. 2019. How Gastrin-Releasing Peptide Opens the Spinal Gate for Itch.
706 *Neuron* **103**:102–117. doi:10.1016/j.neuron.2019.04.022
707 Paige C, Plasencia-Fernandez I, Kume M, Papalampropoulou-Tsiridou M, Lorenzo LE, David ET,
708 He L, Mejia GL, Driskill C, Ferrini F, Feldhaus AL, Garcia-Martinez LF, Akopian AN, De
709 Koninck Y, Dussor G, Price TJ. 2022. A Female-Specific Role for Calcitonin Gene-Related
710 Peptide (CGRP) in Rodent Pain Models. *Journal of Neuroscience* **42**.
711 doi:10.1523/JNEUROSCI.1137-21.2022
712 Palmiter RD. 2018. The Parabrachial Nucleus: CGRP Neurons Function as a General Alarm. *Trends*
713 *Neurosci*. doi:10.1016/j.tins.2018.03.007

714 Park TJ, Comer C, Carol A, Lu Y, Hong HS, Rice FL. 2003. Somatosensory organization and
715 behavior in naked mole-rats: II. Peripheral structures, innervation, and selective lack of
716 neuropeptides associated with thermoregulation and pain. *Journal of Comparative Neurology* **465**.
717 doi:10.1002/cne.10824
718 Park TJ, Lu Y, Jüttner R, Smith ESJ, Hu J, Brand A, Wetzel C, Milenkovic N, Erdmann B,
719 Heppenstall PA, Laurito CE, Wilson SP, Lewin GR. 2008. Selective inflammatory pain
720 insensitivity in the African naked mole-rat (Heterocephalus glaber). *PLoS Biol* **6**.
721 doi:10.1371/journal.pbio.0060013
722 Pauli JL, Chen JY, Basiri ML, Park S, Carter ME, Sanz E, Stanley Mcknight G, Stuber GD, Palmiter
723 RD. 2022. Molecular and anatomical characterization of parabrachial neurons and their axonal
724 projections. *Elife* **11**. doi:10.7554/ELIFE.81868
725 Perner C, Flayer CH, Zhu X, Aderhold PA, Dewan ZNA, Voisin T, Camire RB, Chow OA, Chiu
726 IM, Sokol CL. 2020. Substance P Release by Sensory Neurons Triggers Dendritic Cell
727 Migration and Initiates the Type-2 Immune Response to Allergens. *Immunity* **53**:1063-1077.e7.
728 doi:10.1016/j.immuni.2020.10.001
729 Pinho-Ribeiro FA, Verri WA, Chiu IM. 2016. Nociceptor Sensory Neuron–Immune Interactions in
730 Pain and Inflammation Modulation of Pain Sensitivity by Immune Cells. *Trends Immunol* **xx**.
731 Pojawa-Gołąb M, Jaworecka K, Reich A. 2019. NK-1 Receptor Antagonists and Pruritus: Review of
732 Current Literature. *Dermatol Ther (Heidelb)*. doi:10.1007/s13555-019-0305-2
733 Rogoz K, Lagerström MC, Dufour S, Kullander K. 2012. VGLUT2-dependent glutamatergic
734 transmission in primary afferents is required for intact nociception in both acute and persistent
735 pain modalities. *Pain* **153**. doi:10.1016/j.pain.2012.04.017
736 Russo AF. 2017. Overview of neuropeptides: awakening the senses? *Headache* **57**:37.
737 doi:10.1111/HEAD.13084

738 Salmon AM, Damaj I, Sekine S, Picciotto MR, Marubio L, Changeux JP. 1999. Modulation of
739 morphine analgesia in alphaCGRP mutant mice. *Neuroreport* **10**:849–854.
740 doi:10.1097/00001756-199903170-00033
741 Salmon AM, Damaj MI, Marubio LM, Epping-Jordan MP, Merlo-Pich E, Changeux JP. 2001.
742 Altered neuroadaptation in opiate dependence and neurogenic inflammatory nociception in
743 αCGRP-deficient mice. *Nature Neuroscience 2001 4:4* **4**:357–358. doi:10.1038/86001
744 Scherrer G, Low SA, Wang X, Zhang J, Yamanaka H, Urban R, Solorzano C, Harper B, Hnaskod
745 TS, Edwards RH, Basbaum AI. 2010. VGLUT2 expression in primary afferent neurons is
746 essential for normal acute pain and injury-induced heat hypersensitivity. *Proc Natl Acad Sci U S*
747 *A* **107**. doi:10.1073/pnas.1013413108
748 Sharma N, Flaherty K, Lezgiyeva K, Wagner DE, Klein AM, Ginty DD. 2020. The emergence of
749 transcriptional identity in somatosensory neurons. *Nature 2020 577:7790* **577**:392–398.
750 doi:10.1038/s41586-019-1900-1
751 Sun L, Liu R, Guo F, Wen M qing, Ma X lin, Li K yuan, Sun H, Xu C lin, Li Y yuan, Wu M yin, Zhu
752 Z gang, Li Xin jian, Yu Y qin, Chen Z, Li Xiang yao, Duan S. 2020. Parabrachial nucleus circuit
753 governs neuropathic pain-like behavior. *Nat Commun* **11**:1–21. doi:10.1038/s41467-020-19767-
754 w
755 Tso AR, Goadsby PJ. 2017. Anti-CGRP Monoclonal Antibodies: the Next Era of Migraine
756 Prevention? *Curr Treat Options Neurol* **19**:27. doi:10.1007/s11940-017-0463-4
757 Vandewauw I, De Clercq K, Mulier M, Held K, Pinto S, Van Ranst N, Segal A, Voet T, Vennekens
758 R, Zimmermann K, Vriens J, Voets T. 2018. A TRP channel trio mediates acute noxious heat
759 sensing. *Nature* **555**:662–666. doi:10.1038/nature26137
760 von Euler US, Gaddum JH. 1931. An unidentified depressor substance in certain tissue extracts. *J*
761 *Physiol* **72**:74–87. doi:10.1113/JPHYSIOL.1931.SP002763

762 Warr DG, Hesketh PJ, Gralla RJ, Muss HB, Herrstedt J, Eisenberg PD, Raftopoulos H, Grunberg
763 SM, Gabriel M, Rodgers A, Bohidar N, Klinger G, Hustad CM, Horgan KJ, Skobieranda F.
764 2005. Efficacy and tolerability of aprepitant for the prevention of chemotherapy-induced
765 nausea and vomiting in patients with breast cancer after moderately emetogenic chemotherapy.
766 *Journal of Clinical Oncology* **23**:2822–2830. doi:10.1200/JCO.2005.09.050
767 Wilhelms DB, Dock H, Brito HO, Pettersson E, Stojakovic A, Zajdel J, Engblom D, Theodorsson
768 E, Hammar ML, Spetz Holm ACE. 2018. CGRP Is Critical for Hot Flushes in Ovariectomized
769 Mice. *Front Pharmacol* **9**. doi:10.3389/FPHAR.2018.01452
770 Woolf CJ, Mannion RJ, Neumann S. 1998. Null mutations lacking substance: Elucidating pain
771 mechanisms by genetic pharmacology. *Neuron*. doi:10.1016/S0896-6273(00)80487-0
772 Wu Y, Luna MJ, Bonilla LS, Ryba NJP, Pickel JM. 2018. Characterization of knockin mice at the
773 Rosa26, Tac1 and Plekhg1 loci generated by homologous recombination in oocytes. *PLoS One*
774 **13**:e0193129. doi:10.1371/JOURNAL.PONE.0193129
775 Yaksh TL, Jessell TM, Gamse R, Mudge AW, Leeman SE. 1980. Intrathecal morphine inhibits
776 substance P release from mammalian spinal cord in vivo. *Nature* **286**:155–157.
777 doi:10.1038/286155a0
778 Yang D, Jacobson A, Meerschaert KA, Sifakis JJ, Wu M, Chen X, Yang T, Zhou Y, Anekal PV,
779 Rucker RA, Sharma D, Sontheimer-Phelps A, Wu GS, Deng L, Anderson MD, Choi S, Neel
780 D, Lee N, Kasper DL, Jabri B, Huh JR, Johansson M, Thiagarajah JR, Riesenfeld SJ, Chiu IM.
781 2022. Nociceptor neurons direct goblet cells via a CGRP-RAMP1 axis to drive mucus
782 production and gut barrier protection. *Cell* **185**:4190-4205.e25.
783 doi:10.1016/J.CELL.2022.09.024/ATTACHMENT/4531EC32-46F5-476B-BC42-
784 F51A645ECAB6/MMC6.XLSX

785 Zajdel J, Sköld J, Jaarola M, Singh AK, Engblom D. 2021. Calcitonin gene related peptide α is
786 dispensable for many danger-related motivational responses. *Scientific Reports 2021 11:1* **11**:1–9.
787 doi:10.1038/s41598-021-95670-8
788 Zeisel A, Hochgerner H, Lönnerberg P, Johnsson A, Memic F, van der Zwan J, Häring M, Braun E,
789 Borm LE, La Manno G, Codeluppi S, Furlan A, Lee K, Skene N, Harris KD, Hjerling-Leffler
790 J, Arenas E, Ernfors P, Marklund U, Linnarsson S. 2018. Molecular Architecture of the Mouse
791 Nervous System. *Cell* **174**:999-1014.e22. doi:10.1016/j.cell.2018.06.021
792 Zieglgänsberger W. 2019. Substance P and pain chronicity. *Cell Tissue Res.* doi:10.1007/s00441-018-
793 2922-y
794 Zimmer A, Zimmer AM, Baffi J, Usdin T, Reynolds K, König M, Palkovits M, Mezey E. 1998.
795 Hypoalgesia in mice with a targeted deletion of the tachykinin 1 gene. *Proc Natl Acad Sci U S A*
796 **95**. doi:10.1073/pnas.95.5.2630
797